Localized patterns in reaction-diffusion systems

Vladimir K. Vanag and Irving R. Epstein
Department of Chemistry and Volen Center for Complex Systems, MS 015, Brandeis University, Waltham, Massachusetts 02454, USA

(Received 26 February 2007; accepted 29 May 2007; published online 28 September 2007)

We discuss a variety of experimental and theoretical studies of localized stationary spots, oscillons, and localized oscillatory clusters, moving and breathing spots, and localized waves in reaction-diffusion systems. We also suggest some promising directions for future research in this area.
 [DOI: 10.1063/1.2752494]

A localized pattern consists of one or more regions in one state, typically characterized by a set of concentrations, temperature, and/or other variables, surrounded by a region in a qualitatively different state. Such patterns may be stationary or oscillatory, static or moving. They may have potential applications in biological morphogenesis and in technology. For example, blood clotting can be considered as the formation of localized patterns.[1,2] Some neurological disorders, such as epilepsy, are characterized by spatially localized oscillations in the brain.[3] Localized stationary spots have been suggested as components for structureless memory devices.[4–9] Specific interactions between stationary localized spots or oscillons[10] (objects that are stationary in space and oscillatory in time) or between moving localized spots[11,12] in reaction-diffusion systems may provide a basis for future chemical processors in two dimensions (2D) and even in 3D. Here, we present an overview of the wealth of localized patterns that have been observed experimentally in reaction-diffusion systems and give a brief survey of approaches to modeling these phenomena.

I. INTRODUCTION

Spatially distributed chemically reacting systems are capable of generating a remarkable variety of spatiotemporal patterns. The earliest to be studied were the traveling target and spiral waves in the classic Belousov-Zhabotinsky (BZ) oscillating reaction.[13,14] The experimental realization[15,16] of Turing's idea of temporarily stationary, spatially periodic patterns[17] further demonstrated the ability of reaction-diffusion systems to generate complex spatial structure. More recently, several manifestations of the wave instability have led to new patterns, such as standing, packet, and accelerating waves, in systems in which the BZ reaction takes place in a reverse microemulsion.[16,18] Localized patterns represent a new frontier for this branch of pattern formation science. They have been encountered in a number of physical systems and model equations but have only rarely been found in reaction-diffusion systems to date. We shall focus here on localized patterns that are surrounded by a quiescent, or "silent," stationary area that is in a stable steady state. There are, however, a number of other patterns that can be considered as localized, e.g., a region of oscillations within a stationary Turing pattern (or vice versa),[19,20] or morphological line defects in spiral waves.[21] We do not consider wave packets or a single wave in 1D systems to be localized patterns, since all parts of the medium ultimately become involved in the wave propagation process.

Localized structures have evoked considerable interest in physics, where work on solitons goes back nearly four decades[22] and applications to optical communications[23] have provided much impetus. Breathers, another type of localized structure, are receiving considerable attention for their promise in all-optical logic and switching devices and smart materials.[24,25] The first suggestion that localized modes might arise in reaction-diffusion systems can be found in a paper by Koga and Kuramoto,[26] in which the authors describe "a new chemical pattern…which is a propagationless solitary island in an infinite medium." Their one-dimensional simulation of a piecewise linear caricature of the two-variable Fitzhugh-Nagumo model also yielded a breathing mode under some conditions. Dissipative solitons, both stationary and pulsating, were analyzed in detail by Kerner, Osipov, and Muratov[27,28] primarily, as in the case of Koga and Kuramoto, for two-variable reaction-diffusion models with a rapidly diffusing inhibitor, though they used a slightly different name, "autosolitons."

Experimental examples of localized patterns have been found in a wide range of physical systems: localized waves in binary-fluid convection,[29] dissipative solitary states in driven surface waves,[30] localized microstructures in solidification,[31] solitary stripes and clusters in gas discharge systems,[32,33] autosolitons in semiconductors,[27,34] oscillons in granular materials[35] and at a plasma surface,[36] and optical solitons.[37–40] Some of these experiments, e.g., moving spots in 3D gas-discharge systems and semiconductors, can be described by reaction-diffusion equations, and we briefly discuss some of them here.

In the past decade, several experiments on localized patterns have been performed in chemical (or chemical-like) systems. In the next section, we survey these experiments in homogeneous, spatially extended (mainly quasi-2D) systems. These experiments were performed either in a continuously fed unstirred reactor (CFUR), which provides both stationary conditions and gradients of concentrations in the reactive layer (typically a gel) along the feeding direction, or in closed conditions that eliminate the concentration gradients, but which restrict the time of observation and eliminate the

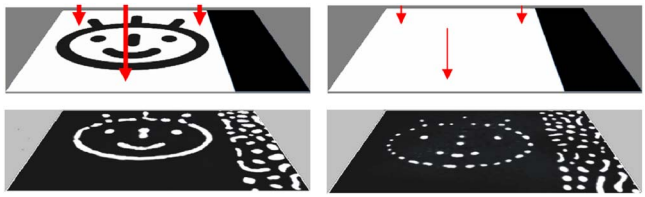

FIG. 1. (Color online) Localized spots in the BZ-AOT system (Ref. 6). (Left column) Illumination of the BZ-AOT reaction through a "face-mask" for 5 min at intensity $I=I_0$ sufficient to suppress all patterns. Right part of the reactor (narrow stripe with Turing stationary spots) remains in darkness. $I_0=28$ mW/cm^2. (Right column) Subsequent illumination without any mask for 1 h at intensity $I=I_0/5$. This intensity of light prevents the emergence of new spots, but cannot suppress already existing patterns. Size of the snapshots is 7.7 mm$\times$5.8 mm. $[\text{Malonic acid}]_0=0.1$ M, $[H_2SO_4]_0=0.3$ M, $[NaBrO_3]_0=0.25$ M, $[Ru(bpy)_3]_0=0.004$ M; volume fraction of aqueous droplets $\varphi_d=0.45$, $\omega\equiv[H_2O]/[AOT]=10$.

possibility of achieving truly stationary conditions. The use of closed systems is feasible only for the BZ, CIMA (chlorite-iodide-malonic acid), and related reactions, in which the dynamic behavior of interest persists for an hour or more. After we describe the observed phenomena, we use these as a basis for further theoretical discussion of various types of models in Sec. III. We then conclude with some general considerations and thoughts about future research directions in this field.

II. EXPERIMENTAL EXAMPLES OF LOCALIZED REACTION-DIFFUSION PATTERNS

We present here examples of several types of localized patterns found in reaction-diffusion systems. Most, but by no means all, of these patterns have been studied in the BZ system, either in a gel reactor (CFUR) or in a closed system in which the reactants are mixed with octane and the surfactant aerosol OT (BZ-AOT system[16,41,42]). After mixing, the system forms a reverse microemulsion that comprises water droplets of diameter $\sim$5–10 nm containing the BZ reactants, surrounded by a monolayer of surfactant molecules and floating in a sea of octane. The average droplet diameter is proportional to the ratio of water to AOT concentrations, while the average spacing between droplets decreases as the [water]:[octane] ratio is raised, until droplets begin to fuse to form water channels.

A. Localized stationary spots

A dramatic example of localized stationary spots is seen in Fig. 1, where we construct a "chemical memory device"[6] using a photosensitive variant of the BZ-AOT system. As the light intensity is varied, the system exhibits a subcritical Turing instability, leading to a regime in which the homogeneous steady state and localized spots can coexist. If we illuminate at high intensity, only the uniform state is stable; in the dark, the sole stable state is the Turing (spot) pattern. We first illuminate at high intensity to establish the uniform state. If we then insert a patterned mask, the dark areas of the pattern are imprinted on the medium. On removing the mask and lowering the light intensity into the bistable range, the imprinted pattern persists for an hour or more. Brief exposure to high-intensity light erases the pattern, but it returns when the light is removed. Longer exposures permanently delete the pattern. Thus, the system can serve as a rewritable memory device.

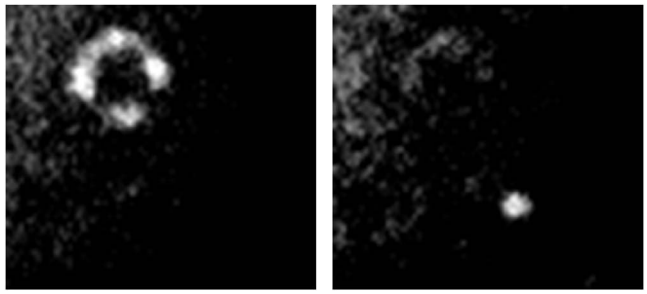

FIG. 2. Oscillon in the BZ-AOT reaction (Ref. 9). The ring diameter is about 0.6 mm. Time between frames, 47 s, is half the period of oscillation. $\varphi_d=0.41$, $\omega\equiv[H_2O]/[AOT]=15$, $[H_2SO_4]=0.25$ M, $[NaBrO_3]=0.2$ M, [MA]=0.25 M, $[Ru(bpy)_3^{2+}]=4.2$ mM. Frame size=2.2$\times$2.0 mm^2.

B. Localized oscillatory spots (oscillons)

An oscillon is a spot, group of spots, or other object that oscillates in time while remaining stationary in space. The term was introduced in plasma physics,[43] but has become more familiar in connection with the striking behavior observed in a thin layer of a vibrated granular material.[35] The first and, to the best of our knowledge, still the only example of oscillons in a chemical system was found in the BZ-AOT system catalyzed by the same $Ru(bpy)_3$ metal complex employed in the case above of stationary spots, but without illumination.[9] Figure 2 shows two snapshots of an oscillon consisting of a spot and a ring. The snapshots are separated in time by half a period of oscillation. During each period, the localized spot disappears for roughly half the interval and the ring for the other half. Oscillons are related to the oscillatory Turing patterns first found in the BZ-AOT system[44] and later in the CDIMA reaction.[45]

C. Breathing spots

A breathing spot resembles an oscillon in that its diameter varies periodically, but breathers never totally disappear as oscillons do. Breathing spots have been found in the ferrocyanide-iodate-sulfite (FIS) reaction carried out in a CFUR.[46] Figure 3 shows an example of the phenomenon. Unfortunately, this single example of a breather in reaction-diffusion systems is not totally convincing, since at maximum extension the edges of the breather are very close to the boundary of the system, and the breathing behavior might be interpreted as arising from interaction between the front and the system boundary.[47]

In general, one can imagine perturbing a single localized spot with disturbances of different symmetries characterized by the number n of lobes around the perimeter of the circular spot, where we write the perturbation in the form $\exp(in\theta)$, and θ is the polar angle. Figure 4 illustrates four possible perturbations of a circular interface. The breathing spot discussed above corresponds to the case $n=0$ of a circularly symmetric perturbation. Breathers can also arise for the case $n=2$. An example of this type of breathing filament in a gas

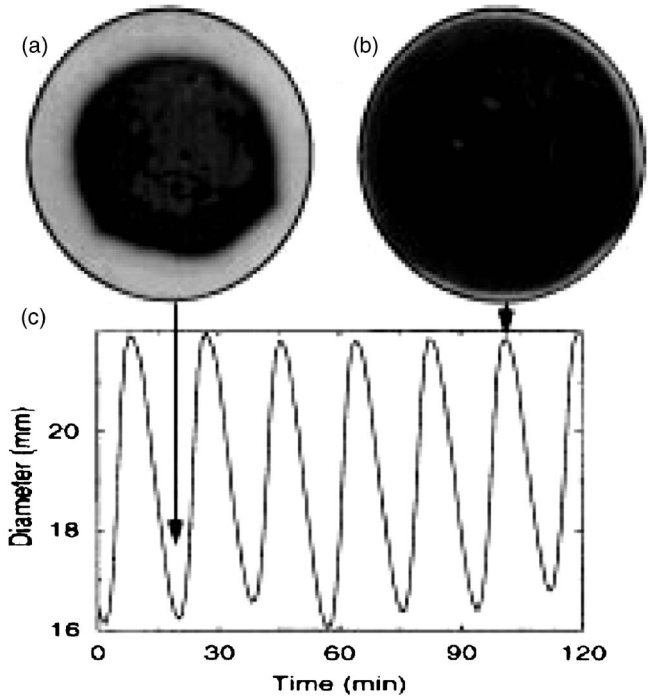

FIG. 3. Breathing spot in the ferrocyanide-iodate-sulfite (FIS) reaction (Ref. 46). (a) Minimal size, (b) maximal size, (c) time evolution of spot diameter. Feeding chamber contains $[H_2SO_4]=3.35$ mM, $[IO_3^-]=75$ mM, $[SO_3^{2-}]=89$ mM, $[K_4Fe(CN)_6]=20$ mM. Flow rate=179 mL/h.

discharge system[48] is shown in Fig. 5. If the amplitude of the breather becomes too large, it can split into two spots. Examples of such splitting or self-replication are well known both in chemistry[49,50] and in gas-discharge systems (Fig. 6).[51]

D. Localized oscillatory clusters

Localized oscillatory clusters are patterns that, like oscillons, are stationary in space and oscillatory in time, but do not have a particular geometry, typically consisting of two regions oscillating out of phase with one another on a stationary background. Clusters with three or more regions are possible, but rare. Each region may be simply connected or may consist of several disjoint subregions. Oscillatory localized clusters have been observed in the BZ reaction in a CFUR subject to periodic external perturbation or to global negative feedback.[52–54] An example is shown in Fig. 7. The sizes of the oscillatory and quiescent domains can be quite different.

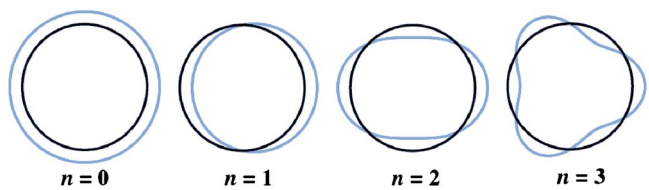

FIG. 4. (Color online) Circular interface (black) subjected to a spatial perturbation (blue) of the form $\exp(in\theta)$.

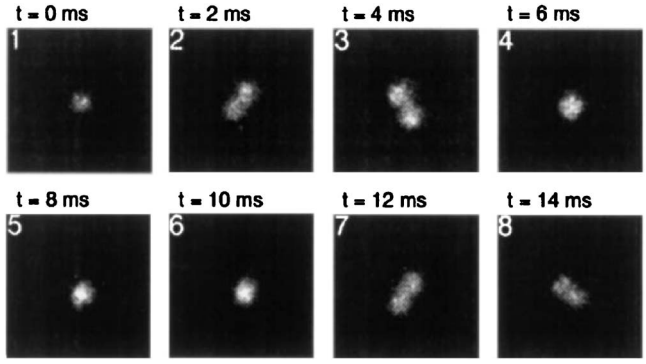

FIG. 5. Breathing filament in a gas discharge system (Ref. 48). Size $\cong 12 \times 12$ mm^2. Diameter of a spot is about 1 mm.

E. Wave segments controlled by global negative feedback

Global negative feedback can lead not only to cluster formation[52] in spatially extended reaction-diffusion systems but also to localized wave segments.[55] Showalter and coworkers have shown that in the excitable photosensitive BZ reaction, the propagation of wave segments is strongly dependent on the intensity of illumination (Fig. 8). Since higher-intensity illumination tends to suppress waves, increasing the intensity as the area of a wave segment grows provides a negative feedback that can be used to control the size of the segment. By utilizing this feature, they have been able to achieve exquisite control over the behavior of sets of BZ wave segments subject to carefully chosen global and local-global feedback. With global feedback only, each wave segment propagates along a straight line (Fig. 8). If additional inhomogeneous illumination is added, the BZ wave segments can be programmed to travel along preselected trajectories (Fig. 9).[56]

F. Autonomous wave segments

Autonomous moving segments of waves (see Fig. 10) have been observed in experiments on the oxidation of CO on a catalytic surface consisting of the 110 face of a single crystal of platinum, on which CO molecules and oxygen atoms have been adsorbed from the gas phase.[57] The wave segments, which can be characterized as dissipative solitons,

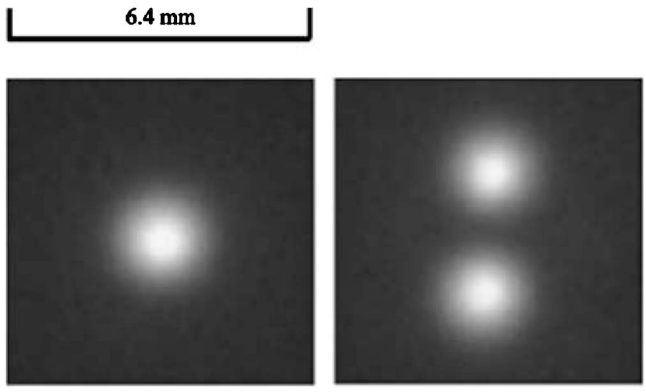

FIG. 6. Splitting of a localized spot in a gas-discharge system (Ref. 51).

FIG. 7. Localized clusters in the photosensitive BZ reaction in a CFUR under global negative feedback (Ref. 52). Concentrations: 1.5 mM of immobilized $Ru(bpy)_3^{2+}$ in a silica gel with thickness $h=0.412$ mm; $[H_2SO_4]_0=0.75$ M, $[NaBrO_3]_0=0.312$ M, $[\text{malonic acid}]_0=0.375$ M, $[NaBr]_0=0.25$ M in the feeding chamber. Size$=7.0\times9.5$ mm^2. Time between snapshots is 37 s (one half-period of oscillation).

were found in a very narrow range of partial pressures of CO and O_2 and temperature $T(\approx 485\,\text{K})$. They move along straight lines parallel to the 001 crystallographic direction at constant velocity $(3.2\ \mu\text{m/s})$. Presumably, the movement of the localized wave segments results from the crystal anisotropy.

G. Moving spots

The translational instability with $n=1$ shown in Fig. 4 corresponds to moving spots. Such localized patterns have been found in semiconductor devices and in gas discharge systems, where a traveling filament was recorded by a streak camera as a single spot.[34] The camera recorded light (infrared recombination radiation) emitted perpendicular to the device plane from the traveling current filament.[58] Figure 11 shows an example of moving spots, as well as their collision and the birth of a new spot.

H. Localized waves

In experiments similar to those described in Fig. 1, we have recently found waves that are confined to localized regions of a photosensitive BZ-AOT system. A thin layer of reactive BZ-AOT microemulsion was illuminated through a striped mask for 3–5 min. Then, after emergence of the first wave, the mask was removed and the intensity of the now homogeneous illumination was decreased. As shown in Fig. 12, waves propagated only in the narrow stripes that had been screened by the mask. The shapes of these dark channels and the paths of the resulting waves can be arbitrarily chosen, so that the waves change their direction according to the shape of the mask. In this fashion, one can establish a connection or communication route between any two points in the system via traveling waves.

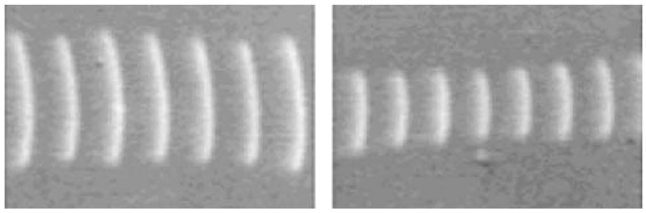

FIG. 8. Superimposed snapshots of a single stabilized wave segment in the photosensitive BZ reaction under homogeneous global negative feedback of intensity I (Ref. 55). The interval between snapshots is 40 s. Frame size is 0.95 cm$\times$1.45 cm. Left and right panels correspond to lower and higher excitabilities, resulting from higher and lower light intensity, respectively. $[NaBrO_3]=0.28$ M, $[\text{malonic acid (MA)}]=0.05$ M, $[\text{BrMA}]=0.165$, $[H_2SO_4]=0.36$ M, silica gel (0.3 mm thickness), $[Ru(bpy)_3^{2+}]=2$ mM. $I=aA+b$, $A=\Sigma_{x,y}\Theta[p(x,y)-p_{\text{th}}]$, p_{th} is a threshold (slightly above the average gray level), Θ is the Heaviside function, $p(x,y)$ is the amplitude of the image at each pixel (x,y).

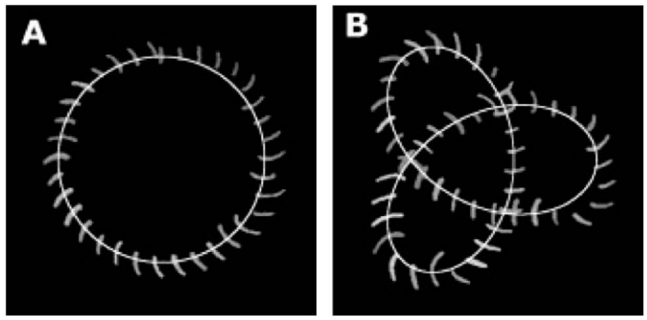

FIG. 9. Two hypotrochoid trajectories, seen as a superposition of snapshots taken every 40 s, of a single wave segment in the BZ reaction controlled by a global negative feedback combined with an additional imposed inhomogeneous illumination whose form confines the wave segment to the chosen trajectory (Ref. 56).

III. MODELS WITH LOCALIZED SOLUTIONS

The number of theoretical and computational works on localized patterns exceeds considerably the number of experimental ones. Nevertheless, a general understanding of the origin and mechanisms of localized patterns is lacking. In

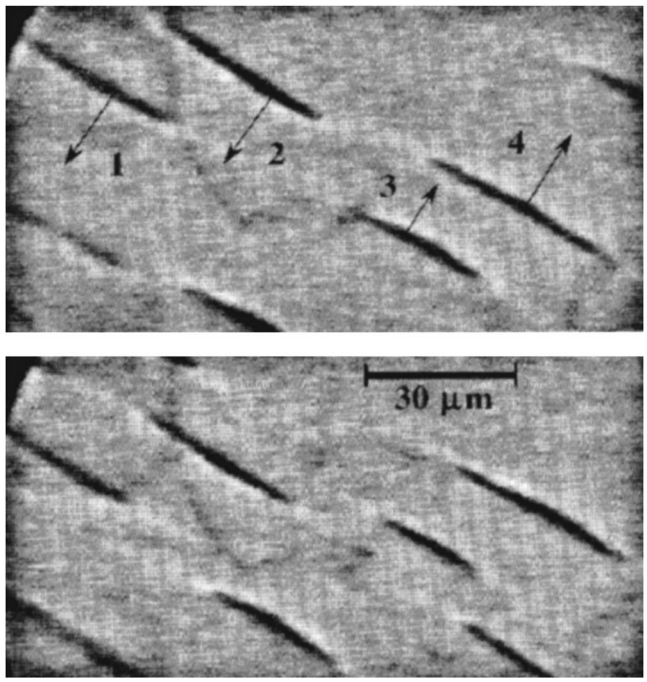

FIG. 10. Two photoemission electron microscopy images taken 3 s apart of a Pt(110) surface during steady-state catalytic CO oxidation. The dark objects (wave segments) are regions with enhanced coverage of adsorbed oxygen atoms. These features move along the indicated directions with constant velocity (Ref. 57). Size$=130\times70\ \mu\text{m}^2$. The width of the pulses is about 2.5 μm; the length is about 30 μm. Pulses of length smaller than 30 μm are not stable.

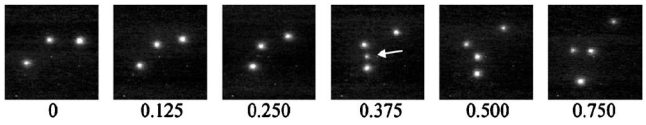

FIG. 11. Moving spots and the birth of a new spot (marked by an arrow) in a gas discharge system (Ref. 58). The time (in s) is indicated at the bottom of each snapshot. Size=14×14 mm^2.

most cases, specific models have been considered without relating them to other models and without attempting to formulate general, simple criteria for the occurrence of localized patterns, such as the requirement that there be an eigenvalue with a positive real part for the Turing or wave instability to arise. Nevertheless, linear stability analysis is applicable to inhomogeneous localized solutions as well as to steady-state and homogeneous solutions.

From experiment and theory, we know that there are different types of localized spots, e.g., stationary spots, breathers, oscillons, and moving spots. What is the controlling parameter and what are the bifurcation scenarios for transitions between these localized spots, or between localized and global patterns? How do localized spots interact with one another? What instabilities are localized patterns subject to? Many other questions await answers. To facilitate thinking about these questions, we present in this section some theoretical models that have been used to generate or explain localized patterns found experimentally. We hope not only to move toward answers to questions about the origin of localized patterns, but also to inspire further experimental questions.

A. Stationary localized spots

Of the various localized patterns, stationary spots have been the most thoroughly studied. Even this "simple" case exhibits a bewildering complexity of behavior. One might, for example, consider the homogeneous behavior of the corresponding 0D model for which the corresponding spatially distributed system gives localized patterns. Such systems can be monostable,[26,27] bistable,[27] or oscillatory.[9,59] In many cases in which localized structures arise, the system is close to a region of bistability in 0D between two steady states[2,26,37,59] or between steady and oscillatory states.[59] The system may be in a region of spatial bistability between homogeneous SS and Turing patterns, a mark of subcritical Turing instability.[5,9,60–63] The most studied cases of localized stationary spots are two-variable activator-inhibitor models with long-range inhibition and short range activation, i.e., where the diffusion coefficient of the inhibitor exceeds that of the activator.

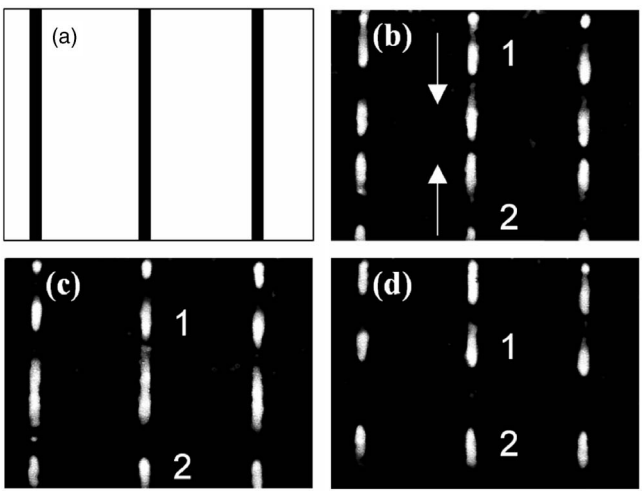

FIG. 12. Localized waves in the BZ-AOT system. (a) Mask. (b)–(d) Snapshots. Time interval Δt between snapshots (b) and (c) is 30 s and Δt=36 s between snapshots (c) and (d). Numbers 1 and 2 mark two approaching waves. Width of the waves is ~0.18 mm. Period is 150 s. $\omega \equiv [H_2O]/[AOT]=12$, $\varphi_d=0.35$, $[H_2SO_4]=0.27$ M, $[NaBrO_3]=0.3$ M, [MA]=0.1 M, $[Ru(bpy)_3^{2+}]=3.6$ mM. Vertical size=5 mm [A. Kaminaga, V. K. Vanag, and I. R. Epstein (unpublished)].

1. Two-variable models with $D_{\text{inhibitor}} > D_{\text{activator}}$

Stationary localized spots are a common solution of two-variable activator-inhibitor or activator-depleted substrate types of models with a fast-diffusing inhibitor (or depleted substrate). Examples include the FitzHugh-Nagumo, two-variable Oregonator, Lengyel-Epstein (LE), Brusselator, and Gray-Scott models.[6,26–28,60,63–69] The general form of such a model is

$$\partial u/\partial t = f(u,v) + \nabla^2 u, \tag{1}$$

$$\partial v/\partial t = g(u,v) + d\nabla^2 v, \tag{2}$$

where ∇^2 is the Laplacian operator ($\partial^2/\partial x^2$ in 1D and $\partial^2/\partial x^2 + \partial^2/\partial y^2$ in 2D); u and v are the activator and inhibitor, respectively, and, in this dimensionless formulation, we take the diffusion coefficients as $D_{\text{activator}}=1$ and $D_{\text{inhibitor}}=d>1$. A localized solution of model (1) and (2) that possesses a single stable steady state at a given set of parameters represents a homoclinic solution.[61] Linear stability analysis of such an inhomogeneous homoclinic solution ($\partial u/\partial t = \partial v/\partial t = 0$) is not an easy problem,[59,70] but can be done in some cases analytically, for example for the Gray-Scott model[61,71] or the Gierer-Meinhardt model.[72]

For 1D FitzHugh-Nagumo-type models, Ohta *et al.*[65,69] wrote Eqs. (1) and (2) in the following form:

$$\varepsilon\tau\partial u/\partial t = \varepsilon^2\partial^2 u/\partial x^2 + f(u) - v, \tag{3}$$

$$\partial v/\partial t = \varepsilon D\partial^2 v/\partial x^2 + \beta u - \gamma v, \tag{4}$$

where all parameters ε, τ, D, β, and γ are positive, $f(u)$ has a cubic-like nonlinearity such as $f(u)=u(u-a)(1-u)$, and $\varepsilon \ll D$. These authors considered the stability of localized patterns (spots) as a problem of stability of the pattern interface. To make the calculations tractable even for this simple case, Ito and Ohta wrote the function $f(u)$ in a piecewise linear form, $f(u)=-u+\Theta(u-a)$, where $\Theta(x)$ is the Heaviside step function.[65] They showed that the boundary of the stationary spot measured by the u profile, the "sharp activator interface," is quite well-defined (Fig. 13). This sharpness allows one to measure the size or the radius R of the localized spot. Ito and Ohta found an analytical solution for R that was strongly dependent on the parameter a. The striking result of their work is that two different solutions, a stationary spot

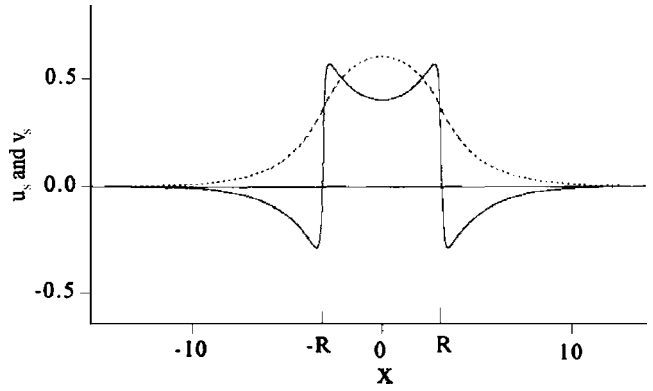

FIG. 13. Localized solution in model (3) and (4) in 1D with $\varepsilon=0.1$, $D=50$, $\gamma=1/3$, $\beta=1$, and $a=0.14$. The width is $R=4.404$. Solid line is u and dashed line is v (Ref. 65).

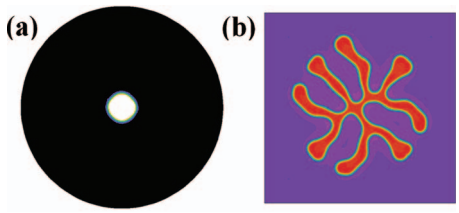

FIG. 14. (Color) Localized spots in model (5) and (6) at $D=0.01$, $a=0.4$, $b=0.2$, $\varepsilon=0.1$, u maps. (a) Outer radius $R=15$, initial circular perturbation with $R_0=1$ expands and quickly reaches a critical radius at which it becomes metastable, but eventually loses circular stability and deforms into a labyrinthine pattern. (b) Total size$=30\times30$. Initial circular perturbation with radius $R_0=10$ shrinks and then slowly transforms to a localized labyrinthine pattern. White and red correspond to $u=-0.2$, black and purple to $u=1$.

and a moving pulse, can coexist at the same set of parameters. Therefore, the form of the localized initial perturbation of the homogeneous steady state (SS) plays a key role in determining the final localized solution. We found very similar behavior experimentally in the BZ-AOT system. The experiments shown in Figs. 1 and 12 were conducted under almost identical conditions, but the result, stationary spots or localized waves, differed from one experiment to another. We note, however, the possibly important difference that our experiments were carried out in 2D, while Ohta *et al.*'s simulations were done on a 1D system.

An alternative approach is to consider the stability of localized spots as a nonequilibrium Ising-Bloch transition[46,73,74] (the equilibrium Ising-Bloch transition has been analyzed in the context of the physics of ferromagnetic systems[75]). Such a treatment is applicable to bistable systems whose two steady states can be connected in space by a stable front. The connecting line, if stationary, is called a heteroclinic orbit or separatrix. For the very simple equation [$a=-1$ for $f(u)$ in Eq. (3)] $u_{xx}+u-u^3=0$, this separatrix can be found analytically as $u_S=\pm\tanh(x/2^{1/2})$.[76]

If a stationary front between two stable SS exists (Ising front),[77,78] then any localized pattern bounded by a pair of these fronts (sometimes referred to as kinks or interfaces) is possible. If the distance between the two interfaces is significantly larger than the characteristic width of the interface, such localized patterns are sometimes called mesas (mesa =table in Spanish). Such patterns with sharp boundaries have been studied in the Brusselator model[66] and in many other models.[27,28,64,79–82] A mesa pattern can lose stability through a Hopf bifurcation of the interface, transforming to a breather if $D_{\text{inhibitor}}$ becomes almost equal to $D_{\text{activator}}$.

If a front between two SS is not stationary (Bloch front), then it moves, and two incoming fronts may approach each other. In this case, a repulsive interaction between two fronts may serve as another mechanism for stabilization of localized patterns. Goldstein *et al.* considered such interactions between fronts in a bistable modified FitzHugh-Nagumo model,[64,83]

$$\partial u/\partial\tau=-u(u-a)(u-1)-b(v-u)+D_u\nabla^2u, \tag{5}$$

$$\partial v/\partial\tau=(-v+u)/\varepsilon+D_v\nabla^2v. \tag{6}$$

The characteristic feature of this modification is that the system always has two stationary SS in 0D, $u_{SS1}=v_{SS1}=1$ and $u_{SS2}=v_{SS2}=0$, separated by an unstable SS, $u_3=v_3=a$. In the limit that $D_v=1/\varepsilon$ and $\varepsilon\to0$ with $D_u=D=\text{const}$, a stationary localized spot solution always exists. We reproduced their simulations and found a localized spot with a very sharp boundary [Fig. 14(a)]. Goldstein *et al.* also showed that such fronts, especially flat fronts, between two steady states can be unstable to transverse perturbation. The resulting labyrinthine pattern is shown in Fig. 14(b). In 1D, the localized spot shown in Fig. 14(a) is stable, since transverse instability cannot occur. Stability analysis of localized patterns with sharp boundaries under global control has been carried out by Pismen.[82]

It has been known since the work of Koga and Kuromoto[26] that bistability is not necessary for localized patterns, but one might suppose that bistability favors localized patterns, since localized patterns are often found in parameter regions close to bistability. Later it was realized that localized stationary patterns (usually spots) can be found in the case of subcritical Turing instability in monostable systems.[63] The condition $D_{\text{inhibitor}}>D_{\text{activator}}$ must also be fulfilled in this case. Goldstein *et al.* in the above-mentioned work[64] underline that neither SS is subject to Turing instability, since $\text{Re}(\lambda)<0$ at all wave numbers k. However, linear stability analysis shows that at some $k_{\max}$ the dispersion curve $\text{Re}(\lambda)$ has a (negative) maximum that is close to $\text{Re}(\lambda)=0$, i.e., to the onset of Turing instability. This case can therefore be considered as a subcritical Turing instability.

The possibility of stationary localized spots and localized hexagonal structures (sets of seven spots) as a result of subcritical Turing instability was shown first in the LE model of the CIMA system.[63] In explaining our experimental result shown in Fig. 1, we also derived a two-variable model, a modification of the Oregonator, that exhibits stationary localized spots both in 1D and 2D,[6]

$$\partial v/\partial\tau=\{[fz+i_0(1-mz)](q-v)/(q+v)+v(1-mz)/(1-mz+\varepsilon_1)-v^2\}/\varepsilon+D_v\nabla^2v, \tag{7}$$

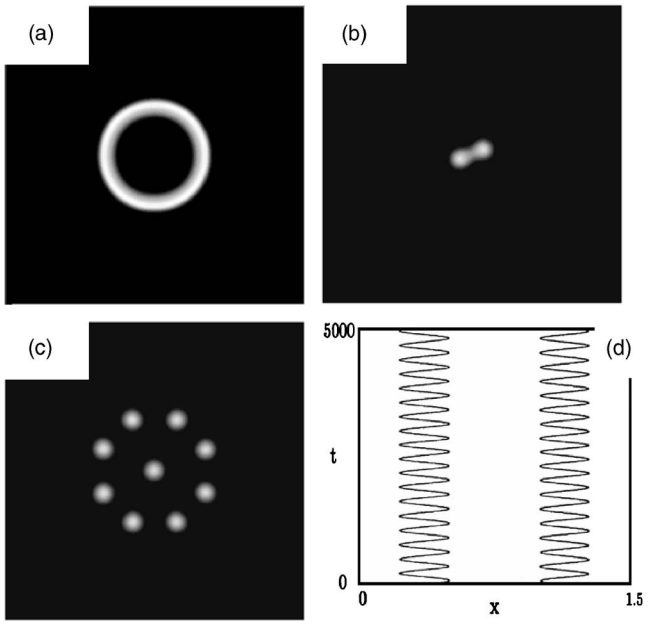

FIG. 15. Instabilities of localized spot. (a) Stationary spot—circular wave transition, (b) splitting, (c) Turing-like, (d) space-time plot for the two interfaces (left and right) of a breather in model (21), (22), and (23b) with $\varepsilon=0.02$, $k=0.5$, $a=600$, $q=0.1$, $r=1.5$, $s=0.145$ (Ref. 101). Snapshots (a)–(c) are from Ref. 6.

$$\partial z/\partial\tau = v(1-mz)/(1-mz+\varepsilon_1) - z + D_Z\nabla^2 z. \tag{8}$$

Varying D_Z and i_0 (the light intensity), we found that a localized spot in 2D may undergo three instabilities: wave emitting, self-replication, and Turing-like, shown in Figs. 15(a)–15(c) respectively. The wave emitting bifurcation (equivalent to pulse generation in 1D) was found in Refs. 6, 65, 84, and 85, self-replication or splitting was observed in Refs. 6, 49, 71, and 86–88, and Turing-like instability of a single spot was reported in Refs. 6 and 63.

2. Stationary spots with equal diffusion coefficients in three-variable models

Recently, localized solutions were found in a model of blood coagulation,[89] which consists of three variables with *equal diffusion coefficients*,[1,59]

$$\partial u_1/\partial t = K_1 u_1 u_2(1-u_1)(1+K_2 u_1)/(1+K_3 u_3) - u_1 + D\nabla^2 u_1, \tag{9}$$

$$\partial u_2/\partial t = u_1 - K_4 u_2 + D\nabla^2 u_2, \tag{10}$$

$$\partial u_3/\partial t = K_5 u_1^2 - K_6 u_3 + D\nabla^2 u_3. \tag{11}$$

Here, u_1 is an activator, u_2 is a second cross activator, and u_3 is the inhibitor. Three SS are possible. One, $u_1=u_2=u_3=0$, is always stationary; the second is a saddle point; and the third can be stationary or Hopf unstable. At $K_1=6.85$, $K_2=13.5$, $K_3=2.36$, $K_4=0.078$, $D=1$, $K_5=27$, and $K_6=0.076$, the third SS is Hopf unstable, and a spatially extended system has a stationary spot solution at equal diffusion coefficients even in 2D. These localized patterns are not consistent with the theories developed by Koga and Kuramoto[26] or by Kerner and Osipov.[27]

As we have seen, there are many different approaches and theories for localized stationary spots, some of them mathematically quite cumbersome. It would be nice to have more qualitative and more general, but less mathematical, explanations. Perhaps such a theory of stationary localized spots might be based on the notion of excitability. A system in a monostable state that is close to a bistable region or to an oscillatory region often exhibits excitability, whereby a perturbation of sufficiently large amplitude results in a large excursion before the 0D system returns to the steady state. In 1D or 2D, such a system may not return, since diffusion may modify the variables in such a way that the system trajectory never reaches a turning point in the phase plane. In the central part of the spot, where the activator concentration lies above the threshold of excitability but below the turning point, the increase in concentration due to the reaction terms is balanced by the losses resulting from diffusion.

In the case of subcritical Turing instability, when the 0D system is not excitable, it may be possible to invoke the idea of a special excitability that exists only in spatially extended systems, as has been suggested for localized spots in an optical cavity filled with a nonlinear Kerr medium.[90,91]

B. Oscillons

We have developed two models for oscillons,[9,10] each of which requires at least three variables. The first model (12)–(14) posits that oscillons arise from interaction between subcritical Turing and subcritical Hopf instabilities,[9]

$$\partial x/\partial t = k_1 - k_2 x - k_4 x + k_5 y x^4/(K^4+x^4) + k_6 y - k_7 x + k_8 z + D_x\nabla^2 x, \tag{12}$$

$$\partial y/\partial t = k_4 x - k_5 y x^4/(K^4+x^4) - k_6 y + D_y\nabla^2 y, \tag{13}$$

$$\partial z/\partial t = k_7 x - k_8 z + D_z\nabla^2 z. \tag{14}$$

The subcritical Turing instability is responsible for the spatial localization, while the subcritical Hopf instability gives rise to the temporal oscillations. Appropriate interaction between the two instabilities can occur only when the regions of wave numbers in which $\mathrm{Re}(\lambda_1)$ has its maximum (Turing instability) and $\mathrm{Im}(\lambda_{2,3})\neq 0$ (Hopf instability) overlap. The system (12)–(14) has two localized solutions, oscillon and stationary spot, at the same set of parameters. Again, the shape of the initial localized perturbation is critical in determining the final solution.

The second model, (15)–(18), which describes the BZ-AOT system, generates 1D oscillons as a result of interaction between subcritical wave and subcritical Hopf instabilities.[10] For some parameter values, these oscillons can move by jumping:

$$\partial x/\partial\tau = [fz(q-x)/(q+x) + x - x^2 - \beta x + s]/\varepsilon + d_x\nabla^2 x, \tag{15}$$

$$\partial z/\partial\tau = x - z - \alpha z + \gamma u + d_z\nabla^2 z, \tag{16}$$

$$\partial s/\partial\tau = (\beta x - s + \chi u)/\varepsilon_2 + d_s\nabla^2 s, \tag{17}$$

$$\partial u/\partial \tau = (\alpha z - \gamma u)/\varepsilon_3 + \nabla^2 u. \quad (18)$$

Similar behavior in 1D occurs in a three-variable modification of the FitzHugh-Nagumo model, which also shows a subcritical wave instability.[92]

Oscillons in 1D were also found in model (19) and (20) with equal diffusion coefficients,[93]

$$u_t = -\mu_1 u - \mu_2 v + \beta_1 u^3 - \gamma u^5 + \nabla^2 u, \quad (19)$$

$$v_t = \mu_2 u - \mu_3 v + \beta_2 u^3 + D\nabla^2 v. \quad (20)$$

While these equations are partial differential equations, it is not clear whether they can be considered reaction-diffusion equations, since they have no direct relation to any chemical or biological reactions. Rather, they are motivated by the quintic complex Ginzburg-Landau equation. For the point system, two solutions, a steady state ($u=v=0$) and an oscillatory state, coexist. At $\mu_1=0.1$, $\mu_2=1.5$, $\mu_3=0.35$, $\beta_1=3$, $\beta_2=1$, $\gamma=2.75$, $D=1$, there are localized oscillations in 1D. However, in 2D this oscillon is unstable, at least at these parameters. Our efforts to vary D and β_1 gave only solutions in which the boundary between the oscillatory and stationary domains moved in one direction or the other.

A spatially localized oscillatory region in 1D was found in a $\lambda-\omega$ model possessing both SS and oscillations (subcritical Hopf instability).[94] In a small 1D region, an analytical solution was obtained for the two-variable Gierer-Meinhardt model,[95] which possesses oscillatory behavior in a narrow range of parameters.[72] It is not clear, however, that such a solution can be classified as localized, since the size L_0 of the region of oscillatory behavior was significantly smaller than the characteristic length L of one of the two variables, $L_0 \ll L$.

C. Breathers

Breathing behavior of the sharp activator interface of a localized spot in 1D was first reported by Koga and Kuramoto.[26] They treated the transition from the stationary to the oscillatory regime of a spot boundary as a Hopf bifurcation. Further investigations of breathers employed a variety of different models, but the general approach of viewing the behavior as arising from supercritical Hopf bifurcation of the spot interface remained unchanged.[26,46,66,71,96–102] Generally, to obtain a breather from a stationary spot one needs to decrease the diffusion coefficient of the inhibitor, though $D_{\text{inhibitor}}$ remains larger than $D_{\text{activator}}$. As noted above, a mesa localized pattern can lose stability through Hopf bifurcation, transforming to a breather as $D_{\text{inhibitor}}$ approaches $D_{\text{activator}}$ (see also Refs. 28, 47, and 103).

In Fig. 15(d), we show breathing of a 1D spot in the three-variable model,[101]

$$\partial u/\partial t = \varepsilon^2 \partial^2 u/\partial x^2 + f(u) - v - w + k, \quad (21)$$

$$a(1-q)\partial v/\partial t = \partial^2 v/\partial x^2 + r(1-s)u - v, \quad (22)$$

$$aq\partial w/\partial t = D\partial^2 w/\partial x^2 + rsu - w, \quad (23a)$$

where $f(u)=u-0.008u^3$. The diffusion coefficient D is assumed to be so large that $w(x,t)$ on a finite interval ($0<x<L$) with zero-flux boundaries becomes homogeneous, i.e., $w(t)$, and Eq. (23a) can be averaged over space (x),

$$aq\mathrm{d}w/\mathrm{d}t = rs\langle u\rangle - w. \quad (23b)$$

We have chosen this model, which has one activator (u) and two inhibitors (v and w), since we will later examine an analogous model for moving spots.

Recent analytical and numerical investigations of breathers in 2D for a three-variable model with one activator and two inhibitors [model (24)–(26)] were made by Gurevich *et al.*[98] This work contains a good review on breathers as well as a study of the bifurcation scenario for the transition from a stationary spot to a breather or to a moving spot (drift mode with $n=1$ in Fig. 4).

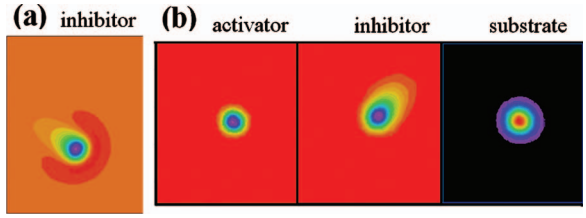

FIG. 16. (Color) (a) Fast inhibitor-map snapshot of a moving spot in model (24)–(26). Parameters: $\lambda=2$, $k_1=7$, $k_3=1$, $k_4=8.5$, $K_w=1$, $\varepsilon=0.02$, $D_u=0.45$, $D_v=0.1$, $D_w=50$, vertical size=6. (b) Moving spot in model (27)–(29). Parameters: $f_0=0.05$, $f_1=0.065$, $f_2=0.5$, $f_3=0.2$, $\tau=100$, $D_u=2.0\times10^{-4}$, $D_v=1.0\times10^{-4}$, $D_w=5.0\times10^{-6}$. Vertical size=1.63. Red (blue-purple) color corresponds to the smallest (largest) concentration.

D. Moving spot

One of the earliest suggestions that moving spots could occur in 2D reaction-diffusion systems was made by Zaikin,[104] and a general analysis of the bifurcation from stationary to moving spots with very thin spot boundaries in 2D was given by Ohta.[81] The most thorough investigations of the dynamics of moving spots, including interaction between spots, have been performed by Purwins and collaborators.[11,105–107]

These latter workers have shown[108,109] that stability of two interacting solitons in a two-variable FitzHugh-Nagumo model requires the introduction of a third, fast-diffusing variable, w, linearly coupled to the activator u and serving as a *second inhibitor*,

$$\partial u/\partial \tau = (\lambda u - u^3 - k_3 v - k_4 w - k_1)/\varepsilon + D_u \nabla^2 u, \quad (24)$$

$$\partial v/\partial \tau = u - v + D_v \nabla^2 v, \quad (25)$$

$$\partial w/\partial \tau = (K_w u - w)/\varepsilon + D_w \nabla^2 w. \quad (26)$$

One may view this second, fast-diffusing inhibitor w as analogous to a global negative feedback, a condition under which we have found localized clusters experimentally[52] and which others[80] have suggested is favorable to localized solutions. Model (24)–(26) has a single SS at parameters where moving spots have been found (see Fig. 16). These parameters [shown in the caption of Fig. 16(a)] are such that $D_w \gg D_u > D_v$. Before asserting that a fast-diffusing second inhibitor is a necessary condition for moving spots, let us look

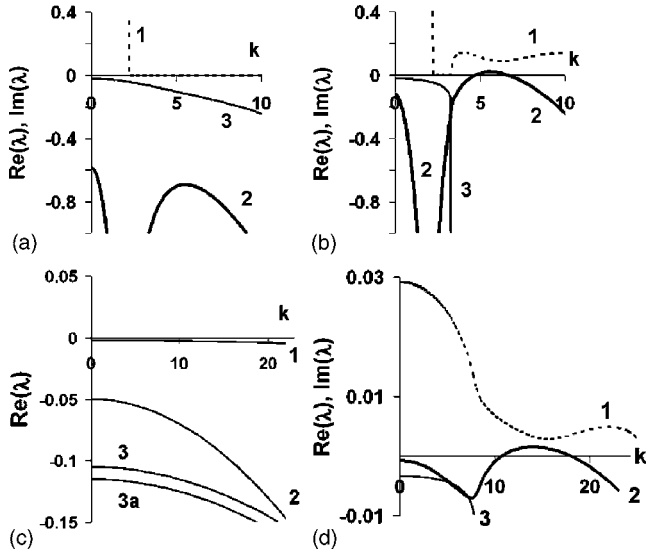

FIG. 17. Dispersion curves [(a), (b)] for model (24)–(26) and [(c), (d)] for model (27)–(29). [(a), (b)] Parameters as in Fig. 16, K_w=(a) 1, (b) 1.35. Dispersion curves for (c) SS1 at f_1=0.055, curve 3, and f_1=0.065, curve 3a, and (d) SS2 at f_1=0.055. All other parameters as in Fig. 16. In (c), all three eigenvalues (curves 1, 2, and 3) are real and negative. In (a), (b), and (d), curve 1 is Im(λ_1), curve 2 is the corresponding Re(λ_1), and curve 3 is the real negative eigenvalue λ_2.

at another model for moving spots proposed recently by Nishiura, Teramoto, and Ueda (model NTU),[12]

$$\partial u/\partial t = f_0(1-u) - uv^2/(1+f_2 w) + D_u \nabla^2 u, \tag{27}$$

$$\partial v/\partial t = uv^2/(1+f_2 w) - (f_0+f_1)v + D_v \nabla^2 v, \tag{28}$$

$$\partial w/\partial t = f_3(v-w)/\tau + D_w \nabla^2 w. \tag{29}$$

Here u is the substrate, v is the activator, and w is the inhibitor, analogous to the fast-diffusing inhibitor w in model (24)–(26). For all parameters, model NTU has a stationary SS at (u=1, v=0, w=0). At some parameters, model NTU may have two additional SS, one of which is stationary, SS2. A moving spot solution [see Fig. 16(b)] exists at parameters for which the system possesses a single SS but lies very close to the bistability region. For these parameters, $D_u > D_v \gg D_w$. Although there is no fast diffusing inhibitor as there is in model (24)–(26), $D_u > D_v$ in both cases. We expect, however, a deeper correspondence between the two models than simply $D_u > D_v$.

To find this similarity, we performed a linear stability analysis of both models. The dispersion curves corresponding to moving spots in models (24)–(26) and (27)–(29) are shown in Figs. 17(a) and 17(c), respectively. In Fig. 17(a), we see that Re(λ) has negative maximum (at k close to 5), which suggests subcritical Turing instability. In model (27)–(29), there is no hint of subcritical Turing instability for SS1 [Fig. 17(c)]. However, small changes in the parameters, for example K_w in model (24)–(26) and f_1 in model (27)–(29), lead to the emergence of a wave instability [Figs. 17(b) and 17(d)]. For model (24)–(26), the wave instability occurs for the same steady state, while for model (27)–(29), the wave instability arises in SS2 [Fig. 17(d)], and the dispersion curve for SS1 remains practically unchanged.

We conclude that both systems (24)–(29) are close to a regime of wave instability and can be considered as systems with a subcritical wave instability. Subcritical wave instability is a plausible explanation for the motion of localized spots. Since wave instability is possible only in systems with at least three variables, this feature explains why three components are necessary for localized moving spots. In system (27)–(29), the "silent" spatial points are in SS1, while the points belonging to the moving spot are in a valley of SS2 and can indeed undergo wave instability.

If one changes the parameters of systems (24)–(29) in the opposite direction, Turing instability can emerge instead of wave instability. Subcritical Turing instability probably accounts for spot localization. Interaction between subcritical Turing and wave instabilities is presumably responsible for the entire phenomenon of moving localized spots.

An analog of a moving spot in reaction-diffusion equations is a *glider* in a cellular automaton.[110,111] A glider solution also requires at least three possible states for each cell of the automaton, which can be interpreted as substrate S, activator E, and inhibitor I. This interpretation comes from the rules of cell transformation.

E. Oscillatory localized clusters

The oscillatory localized clusters[52–54,112] found in experiments involving global negative feedback (see Fig. 7) can be viewed as having three oscillatory regions: two oscillate out of phase and at large amplitude, while the third one has a very small amplitude and is indistinguishable in the experiment from a silent or steady-state region.[53] It is not clear why a homogeneous reactive layer becomes self-organized in such a fashion at a particular value of the global negative feedback strength. In particular, the possible role of small initial perturbations in determining the shapes of the regions, which vary from "identical" experiment to experiment, is unknown.

Rotstein *et al.*[52–54,113–116] invoked the canard phenomenon as a possible origin of localized clusters. They studied a system of identical, discrete, globally coupled relaxation oscillators for which each uncoupled oscillator undergoes a rapid change in the amplitude of its limit cycle (canard) as a parameter is varied. They showed that for a critical value of the global coupling parameter, the network spontaneously partitions itself into sets of low- and high-amplitude oscillators. Both BZ and FitzHugh-Nagumo models were studied, but the generality of this route to localized clusters remains to be established.

F. Interaction between localized patterns

With the exception of studies of a gas-discharge system,[58] there have been no direct experimental investigations of interactions between localized patterns in reaction-diffusion systems. There are, however, several theoretical papers on this subject.[9,10,12,111,117] Nishiura *et al.*[12] found three modes of behavior for interacting moving spots: repulsion, fusion+drift, and annihilation. Schenk *et al.*[117] demonstrated that three or more localized spots can form stable groups of spots at particular interspot distances. Two interacting

oscillons[9] can, depending on the distance between them, give rise to a variety of behaviors including annihilation, the birth of a new oscillatory or stationary spot between the two oscillons, three in-phase oscillons, two in-phase oscillons, two antiphase oscillons, or two stationary spots. Such interactions between localized patterns could potentially be used as logic elements in a "chemical computer."

IV. DISCUSSION, MECHANISMS, OPEN QUESTIONS, AND FUTURE EXPERIMENTS

Two types of diffusive instabilities, the Turing and the wave instability, can render a homogeneous system unstable to an infinitesimal inhomogeneous perturbation. It is sufficient to take into account only linear terms to obtain either the Turing or the wave instability. However, the mechanism of stabilization of the resulting stationary Turing patterns or standing waves requires nonlinear terms and is quite different from the mechanism of instability of the homogeneous SS. These mechanisms can operate independently of one another. For example, if we have a stationary inhomogeneous structure (Turing pattern) and change parameters to push the system to the onset of instability and even beyond, where the homogeneous SS is stable, the existing Turing pattern may survive. In this case, the Turing instability is subcritical. A wave instability may also be subcritical. If we push such a system too far beyond the onset of instability, the original patterns disappear. There is, however, a range of parameters, the region of spatial bistability, for which both the homogeneous SS and stationary or moving patterns are stable.

Now consider the problem from the other side, starting from a homogeneous SS. If the system is in the spatial bistability domain, then we must apply a perturbation of appropriate shape and sufficient amplitude in order to cause a transition to (possibly localized) inhomogeneous patterns stationary either in space or in time. Mechanisms that require finite perturbation of homogeneous SS can be found in a number of experimental and model bistable systems.[64,118–120]

A key problem in understanding localized patterns is to find a mechanism for stabilization of a growing amplitude disturbance in a localized region. Ginsburg-Landau equations or amplitude equations, which have yielded many insights into other pattern formation phenomena in reaction-diffusion systems, do not seem applicable here, since these equations work well only close to the steady state, while localized patterns involve large-amplitude distortions of that state. A novel theoretical approach appears to be required.

The experimental exploration of localized patterns is still at a relatively primitive stage. Clear experimental evidence for breathers in reaction-diffusion systems is lacking, though some preliminary indications of such behavior have been obtained in the chlorine dioxide-iodine-malonic acid reaction in a gel reactor.[121] Moving localized spots in chemical systems also await discovery. Interaction between two or more neighboring oscillons has not been studied experimentally. It should be possible to generate oscillons in proximity to one another by utilizing a photosensitive system, such as the ruthenium bipyridyl-catalyzed BZ-AOT system, and a patterned light source to set the initial conditions. Global negative feedback can be applied to regulate the number of localized spots, as well as to modulate the interaction between localized spots.

No experiments have yet been performed on localized patterns in 3D, where one might expect new types of patterns to arise. If we consider utilizing localized patterns in a new class of chemical computers, then only by employing a 3D configuration is one likely to be able to encode enough information to obtain an advantage over conventional electronic computers. One may speculate whether such a mechanism—interaction among localized patterns in a three-dimensional environment—is already employed in the brains of living organisms.

ACKNOWLEDGMENTS

This work was supported by the donors of the Petroleum Research Fund of the American Chemical Society and by the Chemistry Division of the National Science Foundation. We thank our many collaborators, including Igal Berenstein, Milos Dolnik, Akiko Kaminaga, Horacio Rotstein, Lingfa Yang, and Anatol Zhabotinsky, for their contributions to much of the work described here.

[1] E. S. Lobanova, E. E. Shnol, and F. I. Ataullakhanov, Phys. Rev. E **70**, 032903 (2004).
[2] E. S. Lobanova and F. I. Ataullakhanov, Phys. Rev. Lett. **91**, 138301 (2003).
[3] P. Jung and J. Milton, *Epilepsy as a Dynamical Disease* (Springer, New York, 2003).
[4] S. Barland, J. R. Tredicce, M. Brambilla, L. A. Lugiato, S. Balle, M. Giudici, T. Maggipinto, L. Spinelli, G. Tissoni, T. Knodl, M. Miller, and R. Jager, Nature **419**, 699 (2002).
[5] P. Coullet, C. Riera, and C. Tresser, Chaos **14**, 193 (2004).
[6] A. Kaminaga, V. K. Vanag, and I. R. Epstein, Angew. Chem., Int. Ed. **45**, 3087 (2006).
[7] B. Schapers, M. Feldmann, T. Ackemann, and W. Lange, Phys. Rev. Lett. **85**, 748 (2000).
[8] M. Tlidi, P. Mandel, and R. Lefever, Phys. Rev. Lett. **73**, 640 (1994).
[9] V. K. Vanag and I. R. Epstein, Phys. Rev. Lett. **92**, 128301 (2004).
[10] V. K. Vanag and I. R. Epstein, Phys. Rev. E **73**, 016201 (2006).
[11] M. Bode, A. W. Liehr, C. P. Schenk, and H. G. Purwins, Physica D **161**, 45 (2002).
[12] Y. Nishiura, T. Teramoto, and K. I. Ueda, Chaos **15**, 047509 (2005).
[13] A. T. Winfree, Science **175**, 634 (1972).
[14] A. N. Zaikin and A. M. Zhabotinsky, Nature **225**, 535 (1970).
[15] V. Castets, E. Dulos, J. Boissonade, and P. De Kepper, Phys. Rev. Lett. **64**, 2953 (1990).
[16] V. K. Vanag and I. R. Epstein, Phys. Rev. Lett. **87**, 228301 (2001).
[17] A. M. Turing, Philos. Trans. R. Soc. London, Ser. A **237**, 37 (1952).
[18] V. K. Vanag and I. R. Epstein, Phys. Rev. Lett. **88**, 088303 (2002).
[19] S. Bouzat and H. S. Wio, Phys. Lett. A **268**, 323 (2000).
[20] G. Dewel, P. Borckmans, A. Dewit, B. Rudovics, J. J. Perraud, E. Dulos, J. Boissonade, and P. Dekepper, Physica A **213**, 181 (1995).
[21] J. S. Park and K. J. Lee, Phys. Rev. E **73**, 066219 (2006).
[22] N. J. Zabusky and M. D. Kruskal, Phys. Rev. Lett. **15**, 240 (1965).
[23] N. J. Doran and K. J. Blow, IEEE J. Quantum Electron. **19**, 1883 (1983).
[24] Focus issue on "Nonlinear localized modes: Physics and applications," Chaos **13**, issue 2 (2003), edited by Yu. S. Kivshar and S. Flach.
[25] Yu. S. Kivshar and S. Flach, Chaos **13**, 586 (2003).
[26] S. Koga and Y. Kuramoto, Prog. Theor. Phys. **63**, 106 (1980).
[27] B. S. Kerner and V. V. Osipov, *Autosolitons: A New Approach to Problems of Self-Organization and Turbulence* (Kluwer, Dordrecht, 1994).
[28] C. B. Muratov and V. V. Osipov, Phys. Rev. E **53**, 3101 (1996).
[29] J. J. Niemela, G. Ahlers, and D. S. Cannell, Phys. Rev. Lett. **64**, 1365 (1990).
[30] O. Lioubashevski, H. Arbell, and J. Fineberg, Phys. Rev. Lett. **76**, 3959 (1996).

[31]H. Jamgotchian, N. Bergeon, D. Benielli, Ph. Voge, B. Billia, and R. Guerin, Phys. Rev. Lett. **87**, 166105 (2001).
[32]Yu. A Astrov, E. Ammelt, and H.-G. Purwins, Phys. Rev. Lett. **78**, 3129 (1997).
[33]Yu. A. Astrov and Yu. A. Logvin, Phys. Rev. Lett. **79**, 2983 (1997).
[34]F. J. Niedernostheide, B. S. Kerner, and H. G. Purwins, Phys. Rev. B **46**, 7559 (1992).
[35]P. B. Umbanhowar, F. Melo, and H. L. Swinney, Nature **382**, 793 (1996).
[36]L. Stenflo and M. Y. Yu, Phys. Plasmas **10**, 912 (2003).
[37]V. B. Taranenko, G. Slekys, and C. O. Weiss, Chaos **13**, 777 (2003).
[38]N. N. Rozanov, Opt. Spectrosc. **96**, 569 (2004).
[39]N. N. Rozanov, Phys. Usp. **48**, 167 (2005).
[40]N. N. Rozanov, Opt. Spectrosc. **102**, 255 (2007).
[41]V. K. Vanag and D. V. Boulanov, J. Phys. Chem. **98**, 1449 (1994).
[42]I. R. Epstein and V. K. Vanag, Chaos **15**, 047510 (2005).
[43]L. Stenflo and M. Y. Yu, Phys. Fluids B **1**, 1543 (1989).
[44]A. Kaminaga, V. K. Vanag, and I. R. Epstein, J. Chem. Phys. **122**, 174706 (2005).
[45]D. G. Míguez, S. Alonso, A. P. Muñuzuri, and F. Sagués, Phys. Rev. Lett. **97**, 178301 (2006).
[46]D. Haim, G. Li, Q. Ouyang, W. D. McCormick, H. L. Swinney, A. Hagberg, and E. Meron, Phys. Rev. Lett. **77**, 190 (1996).
[47]C. B. Muratov, Phys. Rev. E **55**, 1463 (1997).
[48]I. Muller, E. Ammelt, and H. G. Purwins, Phys. Rev. Lett. **82**, 3428 (1999).
[49]K. J. Lee, W. D. McCormick, J. E. Pearson, and H. L. Swinney, Nature **369**, 215 (1994).
[50]K. J. Lee and H. L. Swinney, Int. J. Bifurcation Chaos Appl. Sci. Eng. **7**, 1149 (1997).
[51]Y. A. Astrov and H. G. Purwins, Phys. Lett. A **358**, 404 (2006).
[52]V. K. Vanag, L. Yang, M. Dolnik, A. M. Zhabotinsky, and I. R. Epstein, Nature **406**, 389 (2000).
[53]V. K. Vanag, A. M. Zhabotinsky, and I. R. Epstein, J. Phys. Chem. A **104**, 11566 (2000).
[54]V. K. Vanag, A. M. Zhabotinsky, and I. R. Epstein, Phys. Rev. Lett. **86**, 552 (2001).
[55]E. Mihaliuk, T. Sakurai, F. Chirila, and K. Showalter, Faraday Discuss. **120**, 383 (2001).
[56]T. Sakurai, E. Mihaliuk, F. Chirila, and K. Showalter, Science **296**, 2009 (2002).
[57]H. H. Rotermund, S. Jakubith, A. von Oertzen, and G. Ertl, Phys. Rev. Lett. **66**, 3083 (1991).
[58]Y. A. Astrov and H. G. Purwins, Phys. Lett. A **283**, 349 (2001).
[59]V. I. Zarnitsina, F. I. Ataullakhanov, A. I. Lobanov, and O. L. Morozova, Chaos **11**, 57 (2001).
[60]P. Coullet, C. Riera, and C. Tresser, Phys. Rev. Lett. **84**, 3069 (2000).
[61]A. Doelman, R. A. Gardner, and T. J. Kaper, Physica D **122**, 1 (1998).
[62]O. Jensen, V. O. Pannbacker, G. Dewel, and P. Borckmans, Phys. Lett. A **179**, 91 (1993).
[63]O. Jensen, V. O. Pannbacker, E. Mosekilde, G. Dewel, and P. Borckmans, Phys. Rev. E **50**, 736 (1994).
[64]R. E. Goldstein, D. J. Muraki, and D. M. Petrich, Phys. Rev. E **53**, 3933 (1996).
[65]A. Ito and T. Ohta, Phys. Rev. A **45**, 8374 (1992).
[66]T. Kolokolnikov, T. Erneux, and J. Wei, Physica D **214**, 63 (2006).
[67]C. B. Muratov and V. V. Osipov, J. Phys. A **33**, 8893 (2000).
[68]C. B. Muratov, Phys. Rev. E **66**, 066108 (2002).
[69]T. Ohta, M. Mimura, and R. Kobayashi, Physica D **34**, 115 (1989).
[70]B. S. Kerner and V. V. Osipov, Sov. Phys. JETP **47**, 874 (1978).
[71]C. B. Muratov and V. V. Osipov, SIAM J. Appl. Math. **62**, 1463 (2002).
[72]V. V. Osipov, Phys. Rev. E **48**, 88 (1993).
[73]H. Ikeda, M. Mimura, and Y. Nishiura, Nonlinear Anal. Theory, Methods Appl. **13**, 507 (1989).
[74]A. Yadav and D. A. Browne, Physica D **219**, 142 (2006).
[75]L. N. Bulaevskii and V. L. Ginzburg, Sov. Phys. JETP **18**, 530 (1964).
[76]P. Coullet, Int. J. Bifurcation Chaos Appl. Sci. Eng. **12**, 2445 (2002).
[77]L. Kramer, G. Gottwald, V. I. Krinsky, A. Pumir, and V. V. Barelko, Chaos **10**, 731 (2000).
[78]J.-A. Sepulchre and V. I. Krinsky, Chaos **10**, 826 (2000).
[79]B. S. Kerner and V. V. Osipov, Sov. Phys. JETP **52**, 1122 (1980).
[80]K. Krischer and A. Mikhailov, Phys. Rev. Lett. **73**, 3165 (1994).
[81]T. Ohta, Physica D **151**, 61 (2001).
[82]L. M. Pismen, J. Chem. Phys. **101**, 3135 (1994).
[83]D. M. Petrich and R. E. Goldstein, Phys. Rev. Lett. **72**, 1120 (1994).
[84]V. V. Osipov and A. V. Severtsev, Phys. Lett. A **227**, 61 (1997).
[85]P. Schutz, M. Bode, and V. V. Gafiichuk, Phys. Rev. E **52**, 4465 (1995).
[86]C. B. Muratov, Phys. Rev. E **54**, 3369 (1996).
[87]W. N. Reynolds, J. E. Pearson, and S. Ponce-Dawson, Phys. Rev. Lett. **72**, 2797 (1994).
[88]W. N. Reynolds, S. Ponce-Dawson, and J. E. Pearson, Phys. Rev. E **56**, 185 (1997).
[89]E. S. Lobanova and F. I. Ataullakhanov, Phys. Rev. Lett. **91**, 138301 (2003).
[90]D. Gomila, M. A. Matias, and P. Colet, Phys. Rev. Lett. **94**, 063905 (2005).
[91]D. Gomila, A. Jacobo, M. A. Matias, and P. Colet, Phys. Rev. E **75**, 026217 (2007).
[92]L. F. Yang, A. M. Zhabotinsky, and I. R. Epstein, Phys. Chem. Chem. Phys. **8**, 4647 (2006).
[93]O. Descalzi, Y. Hayase, and H. R. Brand, Phys. Rev. E **69**, 026121 (2004).
[94]B. Ermentrout, X. Chen, and Z. Chen, Physica D **108**, 147 (1997).
[95]H. Meinhardt and A. Gierer, J. Theor. Biol. **85**, 429 (1980).
[96]S. E. Folias and P. C. Bressloff, Phys. Rev. Lett. **95**, 208107 (2005).
[97]S. E. Folias and P. C. Bressloff, SIAM J. Appl. Math. **65**, 2067 (2005).
[98]S. V. Gurevich, S. Amiranashvili, and H. G. Purwins, Phys. Rev. E **74**, 066201 (2006).
[99]Y. Nishiura and M. Mimura, SIAM J. Appl. Math. **49**, 481 (1989).
[100]A. Hagberg and E. Meron, Nonlinearity **7**, 805 (1994).
[101]M. Suzuki, T. Ohta, M. Mimura, and H. Sakaguchi, Phys. Rev. E **52**, 3645 (1995).
[102]O. Descalzi and H. R. Brand, Phys. Rev. E **72**, 055202 (2005).
[103]C. B. Muratov and V. V. Osipov, Phys. Rev. E **54**, 4860 (1996).
[104]A. N. Zaikin, J. Physical Thought of Russia **1**, 54 (1995).
[105]S. V. Gurevich, H. U. Bodeker, A. S. Moskalenko, A. W. Liehr, and H. G. Purwins, Physica D **199**, 115 (2004).
[106]A. W. Liehr, H. U. Bodeker, M. C. Rottger, T. D. Frank, R. Friedrich, and H. G. Purwins, New J. Phys. **5**, 89 (2003).
[107]A. W. Liehr, A. S. Moskalenko, Y. A. Astrov, M. Bode, and H. G. Purwins, Eur. Phys. J. B **37**, 199 (2004).
[108]M. Bode, A. W. Liehr, C. P. Schenk, and H.-G. Purwins, Physica D **161**, 45 (2002).
[109]C. P. Schenk, M. Or-Guil, M. Bode, and H.-G. Purwins, Phys. Rev. Lett. **78**, 3781 (1997).
[110]E. R. Berlekamp, J. H. Conway, and R. L. Guy, *Winning Ways for Your Mathematical Plays* (Academic, London, 1982), Vol. 2.
[111]A. Adamatzky, A. Wuensche, and B. D. Costello, Chaos, Solitons Fractals **27**, 287 (2006).
[112]L. Yang, M. Dolnik, A. M. Zhabotinsky, and I. R. Epstein, Phys. Rev. E **62**, 6414 (2000).
[113]H. G. Rotstein, N. Kopell, A. M. Zhabotinsky, and I. R. Epstein, J. Chem. Phys. **119**, 8824 (2003).
[114]H. G. Rotstein, N. Kopell, A. M. Zhabotinsky, and I. R. Epstein, SIAM J. Appl. Math. **63**, 1998 (2003).
[115]H. G. Rotstein, A. A. Zhabotinsky, and I. R. Epstein, Phys. Rev. E **74**, 016612 (2006).
[116]H. G. Rotstein and R. Kuske, Physica D **215**, 46 (2006).
[117]C. P. Schenk, P. Schutz, M. Bode, and H. G. Purwins, Phys. Rev. E **57**, 6480 (1998).
[118]K. J. Lee, W. D. McCormick, Q. Ouyang, and H. L. Swinney, Science **261**, 192 (1993).
[119]K. J. Lee and H. L. Swinney, Phys. Rev. E **51**, 1899 (1995).
[120]J. E. Pearson, Science **261**, 189 (1993).
[121]I. Berenstein, Ph.D. thesis, Brandeis University (2005).